Aquatic Toxicology 232 (2021) 105761

Contents lists available at ScienceDirect

Aquatic Toxicology

journal homepage: www.elsevier.com/locate/aqtox

An 'omics approach to investigate the growth effects of environmentally relevant concentrations of guanylurea exposure on Japanese medaka (*Oryzias latipes*)

Erin J. Ussery [a,*], Kristin M. Nielsen [b], Denina Simmons [a], Zacharias Pandelides [a], Chad Mansfield [c], Douglas Holdway [a]

[a] Faculty of Science, Ontario Tech University, 2000 Simcoe St.N., Oshawa, Ontario, L1H 7K4, Canada
[b] University of Texas at Austin Marine Science Institute, 750 Channel View Drive, Port Aransas, TX, 78373, USA
[c] Department of Environmental Science, Center for Reservoir and Aquatic Systems Research, Baylor University, 1 Bear Place #97178, Waco, TX, 76798, USA

ARTICLE INFO

Keywords:
Guanylurea
Metabolomics
Proteomics
Growth
Development
Early life-stage

ABSTRACT

Metformin is a widely prescribed pharmaceutical used in the treatment of numerous human health disorders, including Type 2 Diabetes, and as a results of its widespread use, metformin is thought to be the most prevalent pharmaceutical in the aquatic environment by weight. The removal of metformin during the water treatment process is directly related to the formation of its primary degradation product, guanylurea, generally present at higher concentrations in surface waters relative to metformin. Growth effects observed in 28-day early life stage (ELS) Japanese medaka exposed to guanylurea were found to be similar to growth effects in 28-day ELS medaka exposed to metformin; however, effect concentrations were orders of magnitude below those of metformin. The present study uses a multi-omics approach to investigate potential mechanisms by which low-level, 1 ng · L^{-1} nominal, guanylurea exposure may lead to altered growth in 28-day post hatch medaka via shotgun metabolomics and proteomics and qPCR. Specifically, analyses show 6 altered metabolites, 66 altered proteins and 2 altered genes. Collectively, metabolomics, proteomics, and gene expression data (using qPCR) indicate that developmental exposure to guanylurea exposure alters a number of important pathways related to the overall health of ELS fish, including biomolecule metabolism, cellular energetics, nervous system function/development, cellular communication and structure, and detoxification of reactive oxygen species, among others. To our knowledge, this is the first study to both report the molecular level effects of guanylurea on non-target aquatic organisms, and to relate molecular-level changes to whole organism effects.

1. Introduction

Metformin is a widely prescribed pharmaceutical used to treat a number of human health disorders; most notably, type-2 diabetes and polycystic ovary syndrome (Trautwein et al., 2014 and Tang et al., 2012). Because it is not biotransformed by humans, an estimated 70 % of each dose of metformin is eliminated from the body via renal excretion, after which metformin may enter municipal wastewater streams (Table S1) (Gong et al., 2012; Pentikäinen et al., 1979). In combination with its pervasive use, this has resulted in relatively high concentrations of metformin in wastewater treatment plant (WWTP) influents (up to 100 μg · L^{-1} metformin) and effluents (up to 21 μg · L^{-1}metformin) (Scheurer et al., 2012; Tisler, and Zwiener, 2018), subsequently leading to contamination of global surface waters at concentrations ranging from the high ng · L^{-1} to low μg · L^{-1} range (Tang et al., 2012; Scheurer et al., 2012; Tisler, and Zwiener, 2018).

The removal of metformin from wastewater is directly related to the bacterial formation of guanylurea, the only known recalcitrant degradation product of metformin (Trautwein et al., 2014). Bacterial conversion to guanylurea is thought to occur via double dealkylation of metformin, whereby both methyl groups are removed at the terminal nitrogen (Fig. S1) (Markiewicz et al., 2017). Thus, wastewater treatment processes often lead to concentrations of guanylurea in effluent that exceed those of metformin considerably (Oosterhuis et al., 2013; Blair et al., 2013; Ghoshdastidar et al., 2015; Scheuerer et al., 2012; Tisler, and Zwiener, 2018). In fact, a recent study by Tisler and Zwiener (2018)

* Corresponding author.
E-mail address: erin.ussery@canada.ca (E.J. Ussery).

https://doi.org/10.1016/j.aquatox.2021.105761
Received 6 July 2020; Received in revised form 11 January 2021; Accepted 16 January 2021
Available online 29 January 2021

reported WWTP effluent concentrations of guanylurea as high as 810 μg · L^{-1}, as compared with 6.5 μg · L^{-1} for metformin.

Similarly, several studies have measured guanylurea at much higher concentrations in surface waters (1–20 μg · L^{-1}), relative to metformin (Oosterhuis et al., 2013; Scheuerer et al., 2012). However, Trautwein et al. (2014) found that concentrations of metformin exceeded those of guanylurea by up to 52 times in German surface waters, where guanylurea was ≤ 0.093 μg · L^{-1}.

Regardless of the conditions driving relative abundance, studies consistently show that metformin is among the most frequently detected pharmaceutical compounds concentrations in global surface waters, including seawater (Ebele et al., 2017; Oosterhuis et al., 2013; Blair et al., 2013; Ghoshdastidar et al., 2015; Scheuerer et al., 2012; Tisler, and Zwiener, 2018; Trautwein et al., 2014). In fact, metformin was detected in 89 % of all samples, and at 97 % of study sites in streams from the Southeastern United States, further underscoring the ubiquity of metformin in the aquatic environment (Bradley et al., 2016).

Biotransformation and biodegradation products of pharmaceuticals, like guanylurea, are also expected to be found concomitantly with their parent compounds in the aquatic environment. It is important to note that many pharmaceutical transformation products remain metabolically active, with potential implications for exposed non-target aquatic biota that remain largely unknown, thus it is advantageous to take transformation products of prevalent pharmaceuticals into consideration when evaluating potential risk.

The median concentration of metformin in surface freshwater in North America is estimated to be 0.022 μg · L^{-1} (based on a composite dataset of > 500 measured concentrations), with a maximum reported concentration of 10.1 μg · L^{-1} (de Solla et al., 2016). In a previous study (Ussery et al., 2018), we showed significant effects on the growth of early-life stage (ELS) Japanese medaka (*Oryzias latipes*) developmentally exposed to a range of environmentally relevant waterborne metformin concentrations (0−100 μg · L^{-1}) for 28 days. Results of that study indicate a lowest observable effect concentration (LOEC) of 1 μg · L^{-1} metformin (for effects on growth; Ussery et al., 2018), a value which is well below the maximum measured surface water concentrations in North America (de Solla et al., 2016).

Effects on the growth of 28-day post hatch (DPH) metformin-exposed larvae were accompanied by metabolome and gene expression changes in whole larvae, with implications for lipid homeostasis, cellular energetics, and the developing central nervous system, among others (Ussery et al., 2018). Ussery et al. (2019) reported similar effects on the growth of ELS medaka developmentally exposed to waterborne guanylurea for 28-days. However, the LOEC derived for guanylurea was in the low ng · L^{-1} range, as compared with a LOEC form metformin in the low μg · L^{-1} range (Ussery et al., 2018).

The present study utilizes a multi-omics approach to investigate potential mechanisms by which guanylurea may affect the growth of ELS fish at such low exposure concentrations (relative to metformin). Consequently, all analyses were perfomed on larval medaka exposed to 1 ng · L^{-1} guanylurea (i.e., the LOEC for growth as reported in Ussery et al., 2019) for 28 days. Metabolomics and proteomics datasets were used to inform decisions regarding genes of interest for subsequent qPCR analysis. To our knowledge, the present study is the first to describe the molecular-level effects of guanylurea on non-target aquatic biota, as well as the first to attempt to link these molecular initiating events to whole-organism outcomes.

2. Materials and methods

2.1. Early life stage study experimental design

Metabolomics and proteomics were performed on samples of guanylurea-exposed larvae collected as part of a companion study; thus, we would refer the reader to Ussery et al. (2019) for a detailed description of experimental methods. Briefly, clutches of medaka embryos (female leucophore-free (FLFII) strain) were separated by sex at 118 h post-fertilization (HPF) by extricating males with fluorescing leucophores via fluorescence microscopy (Leica DM 2000 microscope). For the larger study, 118-HPF embryos were randomly assigned to one of five nominal concentrations (100, 32, 10, 3.2 and 1.0 ng · L^{-1}) of waterborne guanylurea (Sigma Aldrich; CAS # 141−83-3), or a control with lab-water only. However, this report focuses specifically on 28-DPH male larval medaka from 1.0 ng · L^{-1} as this was the experimental lowest observed effect concentration in the larger companion study. Ussery et al., 2019 determined the method detection limit (MDL) for Guanylurea to be 0.25 μg · L^{-1}; thus, concentrations < 0.25 μg · L^{-1} are reported as nominal concentrations throughout the present study. Although limitations in our analytical methods prevented us from detecting below 0.25 μg · L^{-1} with the requisite degree of certainty, concentrations below our MDL are still well below those commonly detected in surface waters (and are therefore considered environmentally relevant). Please see Ussery et al., 2019 for detailed analytical method of measuring guanylurea in tank water. Additional information regarding the determination of treatment concentrations can be found in the Supplemental Material.

2.2. Replicates

Prior to RT-qPCR, metabolomics, and proteomic analysis the authors ran ANOVAs between tanks (n = 4) within treatments (control and guanylurea exposed) to rule out any potential tank effects and found no significant difference between tanks ($p > 0.05$). To account for any slight tank variation, the authors combined the tanks (n = 4) within each treatment (control and guanylurea exposed) and larvae were randomly sampled for further analyses (RT-qPCR, metabolomics and proteomics). At the time of RT-qPCR analysis, cost was largely taken into account when determining the sample number for analyses, thus three biological replicates (containing two whole larvae each to ensure enough RNA for anlyses) were analyzed in triplicate per treatment (n = 3). For metabolomics, 8 biological replicates (containing two whole larvae each following Ussery et al., 2018) were used. The remainder of larvae were used for proteomic analysis, 10 biological replicates for control and 9 biological replicates for guanylurea exposed (containing one whole larvae each).

2.3. RT-qPCR

Briefly, RNA was isolated from subsamples of larval fish in PureZOL™RNA Isolation Reagent (Bio-Rad) using a hand-held homogenizer. RNA concentrations and sample purities were determined using a 0.2 mm TrayCell coupled with a Cary 50 Bio UV–vis Spectrophotometer analyzed at 260-nm and a 2000 factor (sample specific factor x virtual dilution factor 9ssRNA = 40 × 50, respectively). RNA quality was reported via RNA quality indicator (RQI), determined using Experion RNA StdSens kits (Bio-Rad), following the manufacturer's protocol.

Genes chosen for RT-qPCR analysis were selected based on literature availability and their relevance to the metabolomics data. Medaka genome sequences were found in the National Center for Biotechnology Information (NCBI) database. Primers were designed and optimized using Primer3 with a product size range of 75–200 bp (Table S3) and purchased in powdered form from Invitrogen. Primers were validated through an 8-point temperature gradient to verify that each annealed at 60 °C and melt peaks were checked to ensure only one product was created. A 4-point primer concentration curve was also run using a 10-fold dilution (100, 10, 1, and 0.1 ng/μL) and tested in triplicate. Reactions were prepared using the iTaq Universal SYBR Green One-Step Kit (Bio-Rad, Mississauga, Ontario) according to the manufacturer's guidelines. Reactions were performed using RNA samples brought to a concentration of 40 ng/μL in TE buffer. A Bio-Rad CFX96 was used for RT-qPCR analysis using the following settings: SYBR/FM; Reverse Transcription Reaction, 10 min at 50 °C; Polymerase Activation and

DNA Denaturation, 1 min at 95 °C; Amplification: Denaturation at 95 °C, 10 s; Annealing/Extension + plate read at 60 °C, 10–30 seconds; Cycles, 45; Melt-Curve Analysis, 65−95 °C with 0.5 °C increments 2–5 seconds/step. Non-template controls were run for all primers to monitor contamination and primer-dimer formation. Only primers with >90 % efficiencies were used in this research. Three biological replicates (containing two whole larvae each) were analyzed in triplicate per treatment (n = 3). Differences in gene expression between treatments were evaluated via statistical analysis of 2-ΔΔCt values.

2.4. Metabolomics

Metabolomics was performed using 28-DPH larvae exposed to either lab water or 1.0 ng · L^{-1} waterborne guanylurea, according to methods described in Bridges et al. (2018). Briefly, 2 larvae were pooled per sample (8 samples per treatment) and were homogenized in cold 2:5:2 chloroform: methanol: Mili-Q™ solution with a motorized pestle, and then centrifuged. The supernatant was spiked with D-27 myristate as an internal standard (IS), and derivatized with methoxyamine in pyridine solution and N-methyl-*N*-trimethylsilyltri-fluoroacetamide (MSTFA) with 1% trimethylchlorosilane (TMCS). Samples were analyzed by gas chromatography-mass spectrometry (GC–MS; Agilent 6890 GC and 5973 MS).

The Agilent Fiehn Retention Time Locking Library (Agilent part # G1676−90000) was used according to the manufacturer's recommendations for metabolite identification. Chromatographic data were processed using the Automated Mass Spectral Deconvolution & Identification System (AMDIS; National Institute of Standards and Technology, Gaithersburg, Maryland), and data was submitted to the Agilent Fiehn library to generate semi-quantitative relative (to the IS) response factors (RF) for metabolites. A suite of fatty acid methyl ester standards was spiked into every 5th sample (n = 3) to allow the AMDIS Retention Index library to account for slight variations in predicted retention times.

2.5. Proteomics

Proteomic analysis was performed using 28-DPH larvae exposed to either lab water or 1.0 ng · L^{-1} waterborne guanylurea, according to methods described in Simmons et al. (2012 and 2017). Briefly, individual larvae (10 lab water and 9 guanylurea) and were homogenized in tris(hydroxymethyl)aminomethane−HCL with a handheld motorized pestle. Whole larvae homogenate proteins were digested via formic acid digestion as described in Simmons et al. (2012). Digests were dried to near dryness in a centrifugal evaporator, and then re-constituted in 20 µL of 95:5 water: acetonitrile with 0.1 % formic acid. 2 µL of the peptide solution was injected to perform separation via reverse phase liquid chromatography on a Zorbax, 300SB-C18, 1.0 × 50 mm 3.5 µm column (Agilent Technologies Canada Inc., Mississauga, Ontario) using an Agilent 1260 Infinity Binary LC (see Simmons et al., 2012). The Agilent 6530 Accurate-Mass Quadrupole Time of- Flight (Q-TOF) was used as the detector in tandem to the Agilent 1260 system (TRACES lab, University of Toronto Scarborough) (instrumental settings are described in the supplemental materials or refer to Simmons et al., 2012). Analytical runs included a solvent blank, peptide standard (H2016, Sigma Aldrich, Oakville, Ontario), and a BSA digest standard (Agilent Technologies Canada Inc., Mississauga, Ontario) injection every 10 samples to monitor any potential baseline, carry over, drift, and sensitivity during the run. Each individual sample was injected once.

Proteins were identified by searching spectral files against the Uniprot Reference Proteome for Japanese medaka (accessed in August 2018; database: DOI: 10.5281/zenodo.4081749 Released 2020−10-09). Spectral files for each larvae homogenate were pooled into groups by treatment, then each group was searched separately using Spectrum Mill Software (Version B.04.01.141) (Simmons et al., 2017). Following settings recommended by the manufacturer for validating results obtained via Agilent Q-TOF mass spectrometer, proteins were manually validated and then accepted when at least one peptide had a peptide score (quality of raw match between the observed and theoretical spectrum) greater than 6 and the percent of the spectral intensity that are accounted for by the theoretical spectrum (%SPI) of greater than 60 %.

2.6. Statistical analysis

Data were analyzed using SigmaPlot (Systat Software Inc.) unless otherwise specified. Normality of all data was confirmed using a Shapiro-Wilk test prior to subsequent statistical analysis. The $\log_2$ fold change values from RT-qPCR analysis were analyzed using a student's *t*-test to determine statistically significant differences in gene expression between control and guanylurea exposed 28-DPH larvae. An α of 0.05 was used to determine statistical significance for all tests.

Metabolomics reports generated using the Agilent Fiehn Retention Time Locking Library were filtered using a proprietary R (v. 2.15.2) program, designed at the University of North Texas (UNT, Denton, TX, USA) according to a variety of filtration criteria for quality control (detailed in Bridges et al., 2018). Metabolites meeting all criteria were included in a two-tailed Welch's *t*-test, to determine statistically significant differences in relative metabolite abundance between the control and guanylurea-treated groups.

Peak intensity tables of identified medaka proteins were uploaded to the MetaboAnalyst 4 Statistical Analysis tool (Chong et al., 2019), using the following steps: 1) missing values were identified and replaced with half of the lowest value in the dataset; 2) data was not filtered; 3) data was normalized using the median and Pareto scaling (Shahmohamadloo et al., 2020); and 4) fold change analysis (using volcano plot) was performed (raw p-value = 0.05, $\log_2$FC > 2). We also performed partial least squares discriminant analysis (PLS-DA) to obtain variable importance in projection (VIP) scores. We used the 10-fold cross validation method in MetaboAnalyst 4 to determine the predictivity (Q2) and goodness of fit (R2) of the model with the first two components. We chose not use a false-discovery-rate (FDR) corrected p-value because the FDR approach used within MetaboAnalyst 4 does not allow for the selection of a relaxed FDR cut-off (i.e. FDR of 0.25), which is more appropriate for discovery-based studies (i.e. we more concerned with loosing valuable information due to false negatives than the potential of including a false positives at this stage in our exploratory study), and in lieu of an FDR correction, we chose to also include PLS-DA VIP scores to identify proteins with strong influence on the data which added more context to our analyses for discovery purposes. Proteins identified as being responsible for the greatest degree of differentiation between experimental groups were kept and identified using the following pipeline: identify the human gene symbols orthologous to medaka proteins using NCBI Protein blast (protein-protein blast, blastp [e = 10^{-5}]) against the reference proteins (refseq_protein) database with Homo sapiens (taxid:9606) as the organism. Genes symbols were input into The Gene Ontology Resource for GO enrichment analysis of biological processes (geneontology.org). The analysis type that was performed using Gene Ontology (GO) was the PANTHER Overrepresentation Test (Released 20,200,728); database: DOI: 10.5281/zenodo.4081749 Released 2020−10-09. The Fisher's exact test with FDR (false discovery rate) correction was used. For parameters that were used in GO enrichment analysis were logFC(>1), p-value < 0.05, and FDR (false discovery rate) < 0.05. A one-tailed variant of Fisher's exact test, also known as the hypergeometric test for over-representation to assess differentially expressed genes between treatment groups.

3. Results

3.1. Metabolites

Shotgun metabolomics successfully identified 82 metabolites (Table S4). The 82 measured metabolites were subsequently compared

between treatment groups. Of those 82 metabolites, 6 metabolites were found to be significant elevated in guanylurea exposed larvae when compared to controls. Male larval medaka exposed to 1.0 ng · L^{-1} waterborne guanylurea from embryo through 28-DPH had significantly altered abundances of various metabolites (*t*-test, $p < 0.05$; Refer to Table S4 for details). Guanylurea exposure significantly increased (*t*-test, $p < 0.05$; Table 1) the abundance of glucose-6-phosphate, panthothenic acid, putrescine, O-phosphocholamine, adenosine-5-monophosphate, and stearic acid, relative to control fish (as indicated by RF values of 1.4, 1.3, 1.1, 1,2, 1.8, and 1,8 respectively).

3.2. Proteins

An unlabelled non-targeted proteomics approach was employed to identify altered protein abundance in larval medaka exposed to guanylurea compared to control larvae. Analysis showed that male larval medaka exposed to 1.0 ng · L^{-1} guanylurea from embryo through 28-DPH had 66 proteins that were significantly altered when compared to control larvae (T-test, $p < 0.05$, Table 2). Of those 66 altered proteins, 39 were shown to be significantly decreased in abundance, while 27 were shown to be significantly increased (Table 2). PLS-DA and VIP score plots ($R2_{Component\ 1} = 0.77$ & $Q2_{Component\ 1} = 0.69$; $R2_{Component\ 2} = 0.89$ & $Q2_{Component\ 2} = 0.69$) (Fig. 1). The 15 proteins that had the greatest influence on the model (top 11 VIP scores, Component 1) were: striated muscle preferentially expressed protein kinase b (Spegb), probable E3 ubiquitin-protein ligase (Herc3), ryanodine receptor 1 (Ryr1), protocadherin beta-16 (Pcdhb16), dynein heavy chain 11, axonemal (Dnah11), zinc finger protein 29 (Znf292), collagen alpha-6(IV) chain (Col4a6), RANBP2-like and GRIP domain-containing protein 8 (Rgpd8), myosin-binding protein C, slow-type (Mybpc1), late secretory pathway protein AVL9 homolog (Avl9), dipeptidyl peptidase 4 (Dpp4). Additionally, the Gene Ontology Enrichment Analysis (geneontology.org) identified 11 biological processes associated with proteins that were significantly decreased in abundance and 8 processes associated with the proteins significantly increased in abundance in guanylurea exposed fish when compared to controls (Tables 3 and 4). Numerous biological processes were shown to be associated with both increased and decreased protein abundances caused by guanylurea abundance including metabolic processes, biological adhesion and regulation, cellular component organization, various cellular processes, cellular signaling, localization, and response to stimulus (Tables 3 and 4). Additional biological processes associated with proteins found to be decreased in guanylurea exposed larvae were developmental processes, multicellular organismal processes and cellular locomotion.

3.3. RT-qPCR

Results of the RT-qPCR analysis revealed a significant downregulation of transcription factor acetyl-CoA carboxylase 2 (*ac2*) in guanylurea exposed male larvae, relative to controls (log_2fold change [Log_2FC] = -0.88; DF = 1, F = 10.25, p = 0.04). Additionally, the expression of very long chain fatty acids protein 1-like (*elo*) was significantly downregulated in exposed male larvae, as compared with controls ([Log_2FC] = -1.53; DF = 1, F = 9.84, p = 0.03). No significant treatment effects ($p > 0.05$) were observed for other genes of interest (β hydroxyacyl-CoA dehydrogenase (*hcd*), HMG-CoA synthesis (*hgs*), glucose-6-phosphate dehydrogenase (*g6p*), and stearoyl-CoA desaturase (*scd*)) (Fig. 2).

Table 1
Metabolites with significantly altered relative abundances detected in 28-day old Japanese medaka exposed to 1.0 ng · L^{-1} guanylurea when compared with controls (full metabolite list in Table S2).

Metabolite	Metformin/Control (RF value)	p-value
D-glucose-6-phosphate	1.4	1.5E-03
pantothenic acid 2	1.3	9.1E-03
putrescine	1.1	3.1E-02
O-phosphocholine	1.2	4.3E-02
adenosine-5-monophosphate	1.8	4.8E-02
stearic acid	1.8	4.8E-02

4. Discussion

We previously demonstrated similar effects on the growth trajectory of ELS medaka following separate 28-day developmental exposures to metformin, and it's primary degradation product, guanylurea (Ussery et al., 2018, 2019). Although outcomes of exposure were similar for both compounds, the LOEC for guanylurea was found to be considerably lower than that of metformin (it is important to note that the LOECs for both compounds were determined to be of environmental relevance). While the present study's main goal was to utilize a multi-omics approach to elucidate potential mechanisms by which developmental exposure to guanylurea decreased growth of Japanese medaka in the single ng · L^{-1} range, the study was also successful in elucidating other potential mechanisms of action (MOA) of guanylurea in ELS fish, described below.

In humans, metformin's accepted MOA is through AMP-activated protein kinase (AMPK), the upstream kinase for the critical metabolic enzymes acetyl-CoA carboxylase (ACC) and HMG-CoA reductase (HRG), which compose the rate limiting steps for fatty acid and sterol synthesis (Bjorklund et al., 2010; Zagorska, 2010; Zhang et al., 1999). The activation of AMPK results in the phosphorylation, and ultimate deactivation, of ACC. When ACC is active, malonyl-CoA is produced, which is the building block for new fatty acids (Mihaylova and Shaw, 2011). It is through this MOA that AMPK is assumed to control lipid metabolism, with phosphorylation of ACC leading to decreased fatty acid synthesis (Li et al., 2011; Mihaylova and Shaw, 2011).

The findings of Ussery et al., 2018 provided further support for this proposed MOA in humans (in the form of altered metabolite abundances downstream of AMPK in metformin-exposed ELS medaka), while also providing evidence to suggest that metformin may affect non-target aquatic biota via this highly conserved molecular pathway (Garcia and Shaw, 2017). The present study provides evidence that guanylurea may also exert effects on ELS fish in a similar manner, albeit at lower effect concentrations (Ussery et al., 2019). Fig. S1 outlines a possible pathway with which guanylurea exposure may illicit various effects in exposed fish including the molecular effects leading to the apical endpoint of stunted growth observed in Ussery et al. (2019) in exposed larval medaka. To note, this is a hypothesized pathway based on the results found in the current research, further investigation is required in order to map a more concrete MOA.

4.1. Dysregulation of fatty acids

ACC (specifically AC2), localized at the mitochondrial membrane, carboxylates acetyl-CoA to malonyl-CoA, inhibiting carnitine palmitoyl transferase 1 (CPT1) and reducing the passage of acyl-CoA into the inner mitochondrial matrix for β-oxidation (Wakil and Abu-Elheiga, 2009). Our RT-qPCR results show a significant downregulation (Log_2FC = -0.88, p = 0.04 in *ac2* in guanylurea exposed larvae when compared to control larvae, likely explaining the stunted growth and dysregulation of fatty acids, such as stearic and pantothenic acid, both seen to be dysregulated in guanylurea exposed larvae. Further, a significant decrease (Log_2FC = -1.53; p = 0.03) in the expression of elongation of very long chain fatty acid protein like-1 (*elo*) was observed in guanylurea exposed larvae, likely contributing to the dysregulation in fatty acid abundance observed in guanylurea fish compared to controls. Dysregulations in FAs has been shown to be associated with serine/threonine kinases, thus the dysregulation in FAs seen in guanylurea exposed larvae likely the explains the increased abundance in the protein DNA-dependent protein kinase catalytic subunit (Prkdc; Log_2FC = 6.25; p = 2.48E-02) and decreased abundance of mitogen-activated protein kinase kinase kinase

Table 2
List of proteins with their human ortholog, gene symbol, protein name, associated Uniprot accession number, log_2fold change (log_2(FC)), and p-values that were differentially abundant in larval medaka exposed to 1.0 ng · L^{-1} guanylurea when compared to control larvae. A positive log_2(FC) value indicates increased abundance, while a negative value indicates decreased abundance.

Gene Symbol	Human ortholog	Protein Name	Uniprot Accession #	Log_2(FC)	p-value
Spegb	SPEC	Striated muscle preferentially expressed protein kinase b	H2LXP8	−11.63	2.74E-03
Herc3	HERC3	Probable E3 ubiquitin-protein ligase	H2LSS1	−10.87	8.92E-03
Pcdhb16	DCHS1	Protocadherin beta-16	H2LH69	−10.67	6.51E-05
Dnah11	DNAH11	Dynein heavy chain 11, axonemal	H2MHV1	−10.66	5.68E-05
Znf292	ZNF292	Zinc finger protein 292	H2MIS0	−10.66	3.21E-02
col4a6	COL4A6	Collagen alpha-6(IV) chain	H2LZX2	−10.11	1.39E-05
Rgpd8	RGPD8	RANBP2-like and GRIP domain-containing protein 8	H2ML69	−10.08	1.08E-06
Avl9	AV19	Late secretory pathway protein AVL9 homolog	H2ME61	−9.66	3.04E-02
Ryr1	RYR1	Ryanodine receptor 1b (skeletal)	H2L660	−9.34	2.81E-05
Neb	NEB	Nebulin	H2M114	−9.05	1.96E-02
Pkp4	PKP4	Plakophilin-4	H2MQF8	−8.84	3.34E-02
Sacs	SACS	Sacsin	H2MCP6	−8.82	1.34E-04
Fat1	FAT1	Protocadherin Fat 1	H2LVT4	−8.73	2.66E-02
Dock5	DOCK5	Dedicator of cytokinesis protein 5	H2MHI8	−8.45	3.93E-03
Ubr4	UBR4	E3 ubiquitin-protein ligase	H2LGQ9	−8.22	3.85E-02
Ift172	IFT172	Intraflagellar transport protein 172 homolog	H2LXJ7	−8.14	4.03E-02
Gbf1	GBF1	Golgi-specific brefeldin A-resistance guanine nucleotide exchange factor 1	H2L6F7	−7.7	4.67E-03
Hspa41	HSPA4	Heat shock 70 kDa protein 4 L	H2L7I3	−7.21	4.74E-02
Plxna3	PLXNA3	Plexin-A3	H2MW36	−7.18	2.54E-02
Sh3tc1	SH3TC1	SH3 domain and tetratricopeptide repeat-containing protein 1	H2M345	−7.17	1.32E-02
Dmxl2	DMXL2	DmX-like protein 2	H2LCH0	−7.08	5.04E-03
Dchs2	DCHS2	Protocadherin-23	H2LWG4	−7.06	3.27E-02
Grid2	GRID2IP	Glutamate receptor, ionotropic, delta 2 (Grid2) interacting protein, a (Delphilin)	H2LZ91	−6.88	2.84E-02
Mcm3ap	MCM3AP	Germinal-center associated nuclear protein	H2MJD5	−6.85	1.34E-02
Ezh2	EZH2	Histone-lysine N-methyltransferase EZH2	H2LD32	−6.35	4.96E-02
Dctn1	DCTN1	Dynactin subunit 1	H2MVD0	−6.16	4.88E-02
Map4k4	MAP4K4	Mitogen-activated protein kinase kinase kinase kinase 4	H2LYN0	−5.95	4.16E-02
Snx17	SNX17	Sorting nexin-17	H2MNW0	−5.87	4.27E-02
Tox4	TOX4	TOX high mobility group box family member 4	H2LY14	−5.84	3.55E-02
Cacna1a	CACNA1A	Voltage-dependent P/Q-type calcium channel subunit alpha-1A	H2MSN6	−5.76	9.57E-03
Cep170b	CEP170B	Centrosomal protein of 170 kDa protein B	H2MRE8	−5.54	2.69E-02
Noc3l	NOC3L	Nucleolar complex protein 3 homolog	H2MYR4	−5.41	4.79E-02
Limkl1a	LIMK1	Serine/threonine-protein kinase PAK 4	H2LC46	−5.35	4.85E-02
Dcps	DCPS	m7GpppX diphosphatase	H2LZE4	−5.22	1.69E-02
Nfe2	NFE2L1	Endoplasmic reticulum membrane sensor	H2MRG6	−5.07	2.28E-02
Slc12a3	SLC12A3	Solute carrier family 12 member 3	H2L428	−5	4.82E-02
Ddx54	DDX54	ATP-dependent RNA helicase	H2LT40	−4.97	1.63E-02
Gldc	GLDC	Glycine dehydrogenase (decarboxylating), mitochondrial	H2L7W3	−4.71	4.40E-02
Usp22	USP22	Ubiquitin carboxyl-terminal hydrolase 22	H2MZA4	−3.61	4.02E-02
Ryr1	RYR1	Ryanodine receptor 1	H2LPL7	11.42	1.36E-02
Dpp4	DPP4	Dipeptidyl peptidase 4	H2LBZ3	10.2	1.04E-02
Mybpc1	MYBPC1	Myosin-binding protein C, slow-type	H2MM13	9.81	1.60E-02
Sptan1	SPTAN1	Spectrin alpha chain, non-erythrocytic 1	H2MBY2	9.78	5.92E-03
Fat4	FAT4	Protocadherin Fat 4	H2N1Z4	9.43	4.34E-02
Tob1	TOB1	Protein Tob1	H2M4C9	8.36	1.09E-02
Npr1	NPR1	Guanylate cyclase soluble subunit alpha-1	H2M894	7.86	3.56E-02
Cacna1e	CACNA1E	Calcium channel, voltage-dependent, R type, alpha 1E subunit a	H2MSC8	7.6	2.62E-02
Abcc9	ABCC9	ATP-binding cassette sub-family C member 9	H2MRJ2	7.55	1.93E-02
Tmem131	TMEM131	Transmembrane protein 131-like	H2MLY1	7.45	8.52E-03
Dync2h1	DYNC2H1	Cytoplasmic dynein 2 heavy chain 1	H2M4S9	7.21	3.35E-02
Prkx	PRKX	cAMP-dependent protein kinase catalytic subunit PRKX	H2N2A0	7.16	4.33E-02
Slc8a1a	SLC8A1	Sodium calcium exchanger 1h	H2LFE5	7.16	6.57E-03
Slc27a2	SLC27A2	Very long-chain acyl-CoA synthetase	H2LDK1	7.11	4.15E-02
Pkhd1l1	PDHD1L1	Fibrocystin-L	H2LV15	7.03	1.38E-02
Adnp2	ADNP2	Activity-dependent neuroprotector homeobox protein 2	H2MAS0	6.95	1.31E-02
Aldoc	ALDOC	Fructose-bisphosphate aldolase C	H2LL29	6.95	1.04E-02
Myo7b	MYO7B	Unconventional myosin-VIIb	H2MLA9	6.42	2.72E-02
Slc17a6b	SLC17A6	Vesicular glutamate transporter 2.1	H2LNX0	6.31	3.49E-03
Camta1	CAMTA1	Calmodulin-binding transcription activator 1	H2MFN5	6.26	1.74E-03
Prkdc	PRKDC	DNA-dependent protein kinase catalytic subunit	H2LLF6	6.25	2.48E-02
Wdr27	WDR27	WD repeat-containing protein 27	H2M4V3	5.89	2.42E-02
Kmt5b	ASH1L	Histone-lysine N-methyltransferase KMT5B	H2L4R0	5.87	6.47E-03
Tkta	TDKT	Transketolase	H2LAX5	5.67	4.07E-02
Trim2	TRIM2	Tripartite motif-containing protein 2	H2LBD6	5.42	2.71E-02
Col1	COL1A1	Collagen alpha-1(I) chain	H2MRA6	4.4	2.33E-02
Tdrd1	TDRD1	Tudor domain-containing protein 1	A9CPT4	3.47	3.31E-02

kinase 4 (Map4k4; $Log_2FC = -5.95$; $p = 4.16E-02$).

As previously mentioned, one of the accepted MOAs of metformin in the treatment of type-2 diabetes is through AMPK, the upstream kinase for the critical metabolic enzymes ACC and HRG which compose the rate limiting steps for fatty acid and sterol synthesis (Bjorklund et al., 2010; Zagorska, 2010; Zhang et al., 1999). *Hgs* catalyzes the formation of HMG-CoA via the condensation of acetyl-CoA and acetoacetyl-CoA (Ordovas, 2009). HMG-CoA is then reduced to mevalonate via

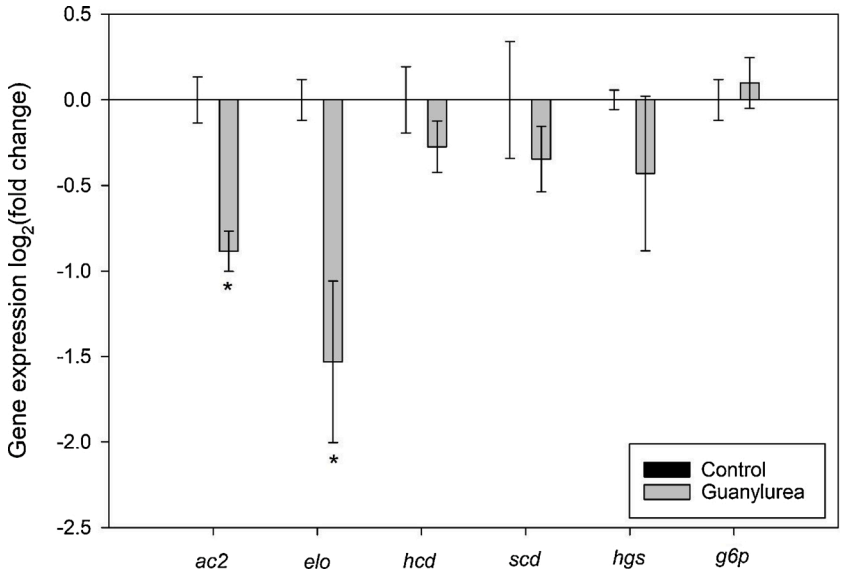

Fig. 1. Mean log_2fold change (± SE) in gene expression between guanylurea exposed and control larvae. An asterisk * denotes significantly altered gene expression relative to controls ($p \leq 0.05$). 2 larvae were homogenized per treatment replicate ($n = 3$ for all groups).

HMG-CoA reductase, the rate limiting step in cholesterol synthesis, a therapeutic pathway metformin takes in for improving the lipid profile (Ordovas, 2009). The authors chose investigate the expression of *hgs* because of its potential involvement in the therapeutic MOA of guanylurea's parent compound, metformin, however no difference in *hgs* expression was observed between treatment groups. Additionally, the authors chose to investigate the expression of *hcd* and *scd* because of their roles in in the MOA of metformin particularly in insulin sensitive and fatty acid synthesis. Metformin's MOA in the activation of AMPK leading to a phosphorylation in TR4 and activation of *scd* which stimulates lipogenesis and increases insulin sensitivity (Kim et al., 2011). Additional research suggests an increase in the expression of *hcd* after metformin treatment leading to an increase in fatty acid β-oxidation (Suwa et al., 2006). Thus, we hypothesized a likely increase in *scd* and *hcd*, which was not observed. A more targeted study design into this pathway is required to fully understand the role of these enzymes in the effects observed in larval medaka exposed to guanylurea.

Similar to AMPK, cAMP-dependent protein kinase catalytic subunit (PRKX) has been shown to phosphorylate ACC in heart tissues (Dyck et al., 1999). The abundance of Prkx was found to be significantly increased ($Log_2FC = 7.16$; $p = 4.33E\text{-}02$) in guanylurea exposed larvae. These increased levels observed in Prkx abundance likely led to increased phosphorylation of *ac2* observed in exposed larvae, resulting in its deactivation and reduced fatty acid biosynthesis.

4.2. Cardio-skeletal myopathies

The remainder of the altered molecular mechanisms observed here do not necessarily follow the accepted MOA of gunaylurea's parent compound, metformin however, they are important to mention. We observed a dysregulation in the abundance of a GTP-related protein, guanylate cyclase soluble subunit alpha-1 (Gucy1a1; $Log_2FC = 7.86$; $p = 3.56E^{-02}$), which is involved in purine metabolism potentially associated with heart dysfunction (Arnold et al., 1977). GUCY1A1 catalyzes the conversion of GTP to 3',5'-cyclic CMP and pyrophosphate (Arnold et al., 1977) and is a primary means of controlling blood flow and thus is important in physiological functions such as smooth muscle relaxation, platelet aggregation, and homeostasis (Isenberg et al., 2009; Rogers et al., 2014). A possible explanation of the increase in abundance in Gucy1a1 in exposed larvae could be explained by the significantly decreased abundance in striated muscle preferentially expressed protein kinase b (SPEG), a novel cardiac myocyte with critical functions in regulating excitation-contraction coupling (Quick et al., 2017; Spegb; $Log_2FC = -11.63$; $p = 2.74E^{-03}$). Although little is known regarding the mechanisms by which altered SPEG levels modulate cardiac function, SPEG mutations have been implicated in centronuclear myophathy, a genetic disease of skeletal and cardiac muscle (Agrawal et al., 2014), thus the increase in the abundance of Gucy1a1 could be associated with the larvae attempting to better regulate blood flow through cardiac muscles. Additionally, the abundance of myosin-binding protein C, slow-type (Mybpc1) was shown to be significantly increased in guanylurea exposed larvae when compared to controls ($Log_2FC = -11.63$; $p = 2.74E^{-03}$). MYBPC1 is a striated muscle protein that regulates contraction in skeletal muscles, and although few studies exist on MYBPC1 it is clear that mutations in this protein cause skeletal myopathies (Leei Lin et al., 2018).

4.3. Glycolysis

Glucose is processed by oxidative catabolism in glycolysis and the pentose phosphate pathway (PPP) in addition to oxidative phosphorylation via the tricarboxylic acid (TCA) cycle in mitochondria (Finelli et al., 2019). Glucose metabolism is essential for proper cell function in numerous pathways such as immune cell function and survival (Maclver et al., 2008), energy homeostasis (Vogt and Bruning, 2013), and proper brain function (Finelli et al., 2019). E3 ubiquitin-protein ligases (HERC3) are shown to promote oxidative glucose metabolism by ubiquitylating and degrading the transcription factor Oct1 which insulates critical target genes against inhibition by oxidative stress, dampens reactive oxygen species (ROS), and promotes glycolytic metabolism (Vazquez-Arreguin et al., 2018). We see a significant decrease in Herc3 abundance in guanylurea exposed larvae when compared to control, possibly associated with the dysregulation in metabolites and proteins related to glucose metabolism ($Log_2FC = -10.87$; $p = 8.92E^{-03}$).

Further, fructose-bisphosphate aldolase C (ALDOC) is an important enzyme in glycolysis converting fructose 1, 6-bisphosphate into glyceraldehyde 3-phosphate which is then converted into pentose phosphate sugars to be used in the PPP by transketolase (TDKT), creating a link between glycolysis and the PPP for the synthesis of energy and nucleotides (Berg et al., 2002). Here, the abundance of both Aldoc ($Log_2FC = 6.95$; $p = 1.04E^{-02}$) and Tdkt ($Log_2FC = 5.67$; $p = 4.07E^{-02}$) were found to be increased in guanylurea exposed larvae when compared to control

Table 3
List of biological processes associated with significantly down-regulated peptides ($p < 0.05$) in GU exposed larval medaka when compared to control larvae.

Biological Process	# of peptides	Associated peptides
Metabolic processes	7	Zinc finger protein 292 (transcription factor), germinal-center associated nuclear protein, endoplasmic reticulum membrane sensor, ATP-dependent RNA helicase, m7GpppX diphosphatase, mitogen-activated protein kinase kinase kinase kinase 4, mitochondrial glycine dehydrogenase (decarboxylating)
Biological adhesion	4	Protocadherin Fat 1, plexin-A3, protocadherin beta-16, plakophilin-4 (intermediate binding protein)
Biological regulation	11	DmX-like protein 2, collagen alpha-6(IV) chain (extracellular matrix structural protein), plexin-A3, zinc finger protein 292 (transcription factor), serine/threonine-protein kinase PAK 4, endoplasmic reticulum membrane sensor, m7GpppX diphosphatase, ryanodine receptor 1b (skeletal), mitogen-activated protein kinase kinase kinase kinase 4, solute carrier family 12 member 3, mitochondrial glycine dehydrogenase (decarboxylating)
Cellular component organization or biogenesis	9	Plexin-A3, serine/threonine-protein kinase PAK 4, protocadherin beta-16, ATP-dependent RNA helicase, intraflagellar transport protein 172 homolog, mitogen-activated protein kinase kinase kinase kinase 4, plakophilin-4 (intermediate filament binding protein), nebulin, solute carrier family 12 member 3
Cellular processes	18	DmX-like protein 2, collagen alpha-6(IV) chain (extracellular matrix structural protein), plexin-A3, zinc finger protein 292 (transcription factor), serine/threonine-protein kinase PAK 4, protocadherin beta-16, endoplasmic reticulum membrane sensor, ATP-dependent RNA helicase, m7GpppX diphosphatase, intraflagellar transport protein 172 homolog, ryanodine receptor 1b (skeletal), mitogen-activated protein kinase kinase kinase kinase 4, axonemal dynein heavy chain 11, nebulin, plakophilin-4 (intermediate filament binding protein), solute carrier family 12 member 3, Voltage-dependent P/Q-type calcium channel subunit alpha-1A, mitochondrial glycine dehydrogenase (decarboxylating)
Developmental processes	4	Plexin-A3, protocadherin beta-16, mitogen-activated protein kinase kinase kinase kinase 4, nebulin
Localization	7	Sorting nexin-17, plexin-A3, germinal-center associated nuclear protein, intraflagellar transport protein 172 homolog, ryanodine receptor 1b (skeletal), Voltage-dependent P/Q-type calcium channel subunit alpha-1A, solute carrier family 12 member 3
Cellular locomotion	1	Plexin-A3
Multicellular organismal processes	4	Plexin-A3, protocadherin beta-16, mitogen-activated protein kinase kinase kinase kinase 4, nebulin
Response to stimulus	3	collagen alpha-6(IV) chain (extracellular matrix structural protein), Plexin-A3, mitogen-activated protein kinase kinase kinase kinase 4
Cellular signaling	4	collagen alpha-6(IV) chain (extracellular matrix structural protein), Plexin-A3, mitogen-activated protein kinase kinase kinase kinase 4,), Voltage-dependent P/Q-type calcium channel subunit alpha-1A

Table 4
List of biological processes associated with significantly up-regulated peptides ($p < 0.05$) in guanylurea exposed larval medaka when compared to controls larvae.

Biological Process	# of peptides	Associated peptides
Metabolic process	7	Tripartite motif-containing protein 2, calmodulin-binding transcription activator 1, protein Tob1, cAMP-dependent protein kinase catalytic subunit, DNA-dependent protein kinase catalytic subunit, guanylate cyclase soluble subunit alpha-1, fructose-bisphosphate aldolase C
Biological adhesion	1	Protocadherin 1
Biological regulation	7	Calmodulin-binding transcription activator 1, protein Tob1, cAMP-dependent protein kinase catalytic subunit, DNA-dependent protein kinase catalytic subunit, guanylate cyclase soluble subunit alpha-1, ryanodine receptor 1a (skeletal), vesicular glutamate transporter 2.1
Cellular component organization or biogenesis	2	Cytoplasmic dynein 2 heavy chain 1, DNA-dependent protein kinase catalytic subunit,
Cellular process	10	Tripartite motif-containing protein 2, cytoplasmic dynein 2 heavy chain 1, calmodulin-binding transcription activator 1, cAMP-dependent protein kinase catalytic subunit, DNA-dependent protein kinase catalytic subunit, guanylate cyclase soluble subunit alpha-1, fructose-bisphosphate aldolase C, ryanodine receptor 1a (skeletal), calcium channel voltage-dependent R type alpha 1E subunit a, vesicular glutamate transporter 2
Localization	5	Cytoplasmic dynein 2 heavy chain 1, ATP-binding cassette sub-family C member 9, ryanodine receptor 1a (skeletal), calcium channel voltage-dependent R type alpha 1E subunit a, vesicular glutamate transporter 2.1
Response to stimulus	3	cAMP-dependent protein kinase catalytic subunit, DNA-dependent protein kinase catalytic subunit, guanylate cyclase soluble subunit alpha-1
Cellular signaling	4	cAMP-dependent protein kinase catalytic subunit, guanylate cyclase soluble subunit alpha-1, calcium channel voltage-dependent R type alpha 1E subunit a, vesicular glutamate transporter 2.1

larvae. The gene, glucose-6-phosphate, found to be increased in guanylurea exposed larvae ($RF = 1.4$; $p = 1.5E^{-03}$), is another intermediate of glycolysis and is used by the PPP for the production of NADPH, which can be consumed by antioxidant enzymes to reduce ROS induced damage (Stanton, 2012). Interestingly, no difference in the expression of *g6p* was observed in guanylurea exposed larvae when compared to controls. We chose to measure *g6p* because of the significant increase in glucose-6-phosphate in larvae exposed to guanylurea when compared to controls as *g6p* is the enzyme in the first reaction of the pentose phosphate pathway which catalyzes the oxidation of glucose-6-phosphate, producing NADPH required for fatty aid synthesis (Bhardwaj, 2013). From this study, however, it is unclear why a significant increase in glucose-6-phosphate was observed, while no difference in *g6p* expression was observed in guanylurea exposed larvae. A more targeted study design into this pathway is required.

Mitochondrial oxidative phosphorylation and generation of adenosine triphosphate (ATP) synthesis is coupled with respiration which produces ROS as by-products of normal cellular metabolism (Ziegler et al., 2015). ROS induced damage was not investigated through this work; however, this remains an area of interest for future studies.

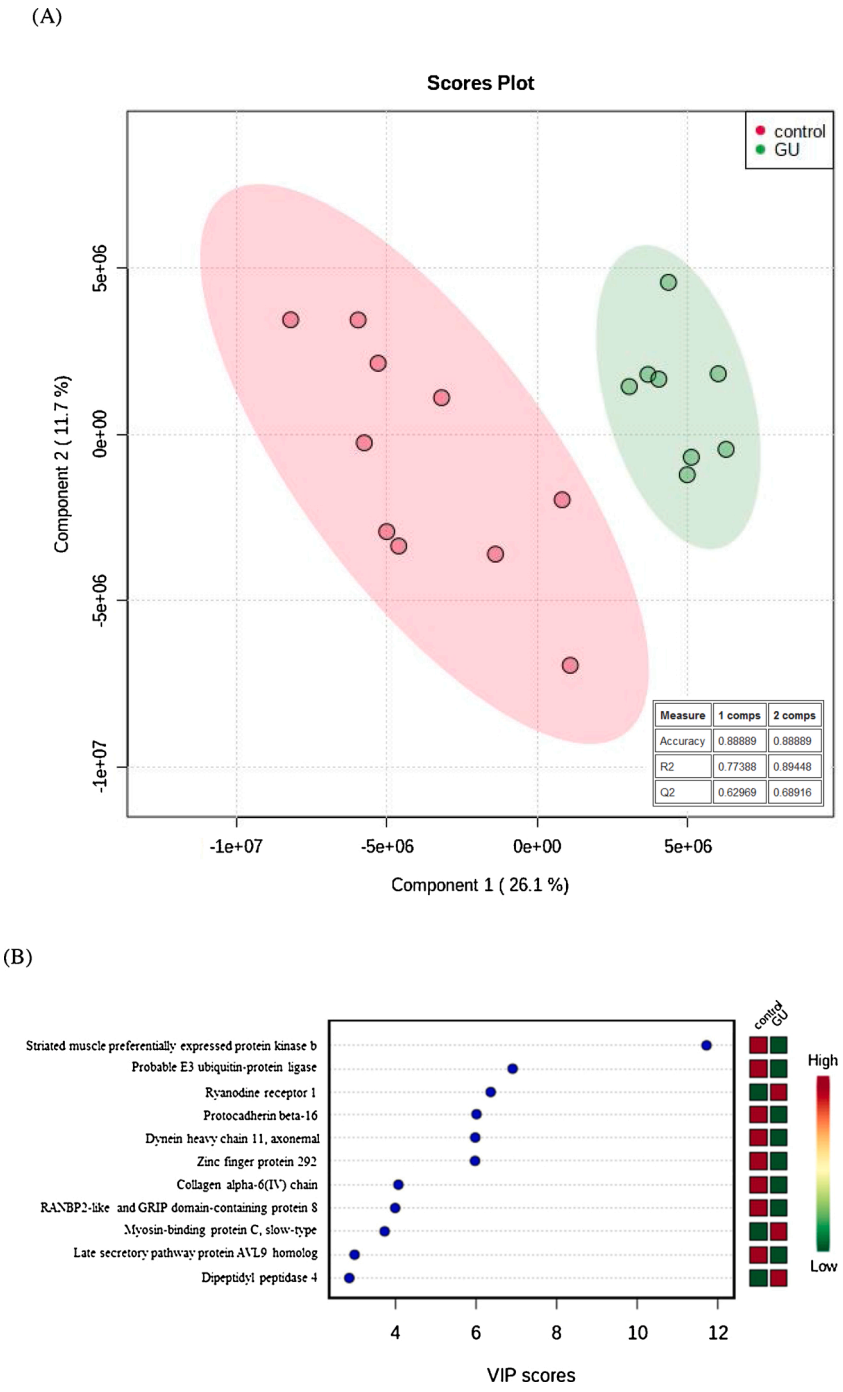

Fig. 2. Partial least squares discriminant analysis (PLS-DA) 2D scores plot of the fitted model with cross validation results of guanylurea (GU, green) and control (red) (panel A), and top 15 variable importance in projection (VIP) scores plot where the coloured boxes on the right indicate protein abundance (panel B) based upon proteins identified in larval Japanese medaka after 28-day early life-stage exposure to 1 ng · L^{-1} GU.

Additionally, it has been shown that high concentrations dysregulated concentrations of glucose and fatty acids may increase the abundance of dipeptidyl peptidase 4 (Dpp4; $Log_2FC = 10.20$; $p = 1.04E^{-02}$), which functions to degrade glucagon-like peptide 1 (GLP-1), which stimulates insulin secretion from β-cells, while DPP4 inhibitors work to enhance glucose-dependent insulin secretion by suppressing GLP-1 degradation (Miyazaki et al., 2012). We observed a significant increased abundance of Dpp4 in guanylurea exposed larvae, which could be explained by the dysregulation in fatty acids and likely dysregulation in glucose metabolism observed in guanylurea exposed larvae.

4.4. Glucose metabolism and cellular function

Glucose metabolism also provides the required energy for cellular function and communication in the brain and participates in balancing the levels of oxidative stress in neurons, with defects in glucose metabolism associated with neurodegenerative diseases (Finelli et al., 2019). Guanylurea exposed larvae showed a dysregulation of the skeletal muscle ryanodine receptor 1b (Ryr1; $Log_2FC = 10.20$; $p = 1.04E^{-02}$) and two important polyamines associated with central nervous system health, putrescine (RF = 1.1; p = 3.1E-02) and o-phosphocolamine (RF = 1.2; p = 4.3E-02). Mutations in skeletal muscle RYR1 has been

associated with neuromuscular disorders such as Malignant Hyperthermia, Central Core Disease and Multiminicore Disease (Treves et al., 2005). An early response to CNS injury is the induction of polyamine (PA) metabolism, resulting in increased levels of putrescine (Adibhatla et al., 2002; Muller et al., 2007), a precursor to higher level PA's found in all eukaryotes (Bridges et al., 2018). O-phosphocolamine is an ethanolamine derivative that is used to construct glycerophospholipid and sphingomyelin (Toda et al., 2017), which play an important role in cell signaling cascades mediating cellular apoptosis, proliferation, stress response, necrosis, and cell differentiation (Bridges et al., 2018; Perry and Hannun, 1998). Although this was not specifically investigated in guanylurea exposed larvae, the potential dysregulation in the aforementioned signaling cascades may lead to developmental defects, autoimmune diseases, neurodegeneration, or cancer (Elmore, 2007), however further investigation is necessary.

4.5. Neuronal communication

The abundance of proteins such as the glutamate receptor ionotropic, delta-2 interacting protein (Grid2ip; $Log_2FC = 6.88$; $p = 2.84E^{-02}$), the vesicular glutamate transporter 2.1 (Slc17a6; $Log_2FC = -6.31$; $p = 3.49E^{-03}$), and the calcium channel, voltage-dependent, R type, alpha 1E subunit (Cacna1e; $Log_2FC = 7.86$; $p = 9.57E^{-03}$) were all significantly different in guanylurea exposed larvae when compared to control larvae, and likely contribute to many of the biological processes associated with neuronal communication altered exposed fish (Tables 3 and 4). GRID2IP, a protein functioning as an excitatory neurotransmitter (Schmid et al., 2009), interacts with SLC17A6 which mediates the uptake of glutamate into synaptic vesicles at presynaptic nerve terminals of excitatory neural cells (Akazome et al., 2011; Pernice et al., 2019). Further, CACNA1E is involved in modulating neuronal firing patterns (Neely and Hidalgo, 2014). Additionally, protocadherins are important for the formation and function of neural circuits which includes dendrite arborization, axon outgrowth and targeting, synaptogenesis, and synapse elimination (Peek et al., 2017) We saw a significant decrease in the abundance of protocadherin beta-16 in guanylurea exposed larvae which could lead to dysregulations in neuronal formation and communication (Pcdhb16; $Log_2FC = -10.67$; $p = 6.51E^{-05}$).Metformin is shown to reduce neurological symptoms in some human patients and reduce neurological disease phenotypes in animal and cell models, by balancing survival and death signaling in cells through pathways that are commonly associated with neurodegenerative diseases (Rotermund et al., 2018). Unfortunately, no research has been done investigating the neurological effects of guanylurea on organisms, further investigation is required.

A few limitations lie within the present exploratory study. First, whole organisms were used to in all three of the various 'omic assessments performed in this study, so we are unable to relate effects to specific organs. Additionally, the study used Japanese medaka as the research organism, which has not yet been fully annotated, particularly in regard to proteins, thus human homologues were used. Future research should consider analyzing 'omic endpoints based on organ (i.e. brain and liver) which would allow for deeper investigation into the MOA of guanylurea on non-target organisms.

5. Conclusion

To our knowledge, the findings of the present study provide some of the first evidence of molecular level developmental effects in ELS fish exposed to environmentally relevant concentrations of guanylurea. Moreover, these effects are observed at concentrations presently measured in the environment. Collectively, findings of our prior related studies (Ussery et al., 2018, 2019) and those reported herein provide additional support for currently proposed MOA for metformin, which demonstrate metformin's conserved effects across taxa, and provide evidence to suggest that guanylurea acts via a similar mechanism. Additionally, the proteomics and metabolomics data presented as part of the present study provide insight to the key molecular initiating events that may lead to higher level adverse effects on nontarget aquatic biota (i.e., assist in development of adverse outcome pathways [AOPs]). Finally, our findings suggest a need for field-based studies aimed at elucidating the possible effects of both chronic metformin and guanylurea exposure on wild fish populations in receiving waters.

CRediT authorship contribution statement

Erin J. Ussery: Conceptualization, Data curation, Formal analysis, Investigation, Writing - original draft. **Kristin M. Nielsen:** Conceptualization, Writing - review & editing. **Denina Simmons:** Investigation, Writing - review & editing. **Zacharias Pandelides:** Investigation, Writing - review & editing. **Chad Mansfield:** Data curation, Formal analysis, Writing - original draft. **Douglas Holdway:** Writing - review & editing, Funding acquisition, Supervision.

Declaration of Competing Interest

The authors report no declarations of interest.

Acknowledgements

The authors would like to thank Dr. Barney Venables for his assistance and guidance with the metabolomics analysis presented in this manuscript. The authors also wish to thank John Guchardi for all of his assistance for any laboratory work pertaining to this publication. We also wish to thank our sources of funding (Canada Research Chairs, Tier 1 #950-221924, NSERC#360557-2011) for the monetary support for this research. We would like to thank the National Institute of Natural Sciences, National BioResource Project (NBRP) and the National Institute of Basic Biology for the FLFII MT109 Japanese medaka strain used for this research. Thank you to Yuko Wakamatsu at Nagoya University, Bioscience and Biotenchnology Center for transferring and submitting the biological materials to NBRP. The authors would also like to sincerely thank Dr. Naomi Stock at the Water Quality Center at Trent University for the analysis of metformin throughout the project.

Appendix A. Supplementary data

Supplementary material related to this article can be found, in the online version, at doi:https://doi.org/10.1016/j.aquatox.2021.105761.

References

Adibhatla, R.M., Hatcher, J.F., Sailor, K., Dempsey, R.J., 2002. Polyamines and central nervous system injury: spermine and spermidine decrease following transient focal cerebral ischemia in spontaneously hypertensive rats. Brain Res. 938, 81–86.

Agrawal, P.B., Pierson, C.R., Joshi, M., Liu, X., Ravenscroft, G., Moghadaszadeh, B., Talabere, T., Viola, M., Swanson, L.C., Haliloglu, G., Talim, B., Yau, K.S., Allcock, R. J.N., Laing, N.G., Perrella, M.A., Beggs, A.H., 2014. SPEG interacts with myotubularin, and its deficiency causes centronuclear myopathy with dilated cardiomyopathy. Am. J. Hum. Genet. 95, 218–226. https://doi.org/10.1016/j.ajhg.2014.07.004.

Akazome, Y., Kanada, S., Oka, Y., 2011. Expression of vesicular glutamate Transporter-2.1 in medaka terminal nerve gonadotrophin-releasing hormone neurones. J. Neuroendocrinol. 23, 570–576. https://doi.org/10.1111/j.1365-2826.2011.02142.x.

Arnold, W.P., Mittal, C.K., Katsuki, S., Murad, F., 1977. Nitric oxide activates guanylate cyclase and increases guanosine 3':5'-cyclic monophosphate levels in various tissue preparations. Proc. Natl. Acad. Sci. U.S.A. 74 (8), 3203–3207.

Berg, J.M., Tymoczko, J.L., Stryer, L., 2002. Biocehmistry, ed 5. W H Freeman and Company, New York.

Bhardwaj, S.B., 2013. Alcohol and gastrointestinal tract function. In: Watson, R.R., Preedy, V.R. (Eds.), Bioactive Food as Dietary Interventions for Liver and Gastrointestinal Disease. https://doi.org/10.1016/C2011-0-07464-1.

Bjorklund, M.A., Vaahtomeri, K., Peltonen, K., Violet, B., Makela, T.P., Laiho, M., 2010. Non-CDK-bound p27 (p27(NCDK)) is a marker for cell stress and is regulated through the Akt/PKB and AMPK-kinase pathways. Exp. Cell Res. 316, 762–774.

Blair, B.D., Crago, J.P., Hedman, C.J., Treguer, R.J.F., Magruder, C., Royer, L.S., Klaper, R.D., 2013. Science of the Total Environment Evaluation of a model for the

removal of pharmaceuticals, personal care products, and hormones from wastewater. Sci. Total Environ. 444, 515–521. https://doi.org/10.1016/j.scitotenv.2012.11.103.
Bradley, P.M., Journey, C.A., Button, D.T., Carlisle, D.M., Clark, J.M., Mahler, B.J., Nakagaki, N., Qi, S.L., Waite, I.R., VanMetre, P.C., 2016. Metformin and other pharmaceuticals widespread in wadeable streams of the southeastern United States. Environ. Sci. Technol. Lett. 3 (6), 243–249.
Bridges, K.N., Zhang, Y., Curran, T.E., Magnuson, J.T., Venables, B.J., Durrer, K.E., Allen, M., Roberts, A.P., 2018. Alterations to the intestinal microbiome and metabolome of Pimephales promelas and Mus musculus following exposure to dietary methylmercury. Environ. Sci. Technol.
Chong, J., Wishart, D.S., Xia, J., 2019. Using metaboanalyst 4.0 for comprehensive and integrative metabolomics data analysis. Curr. Protoc. Bioinformatics 68.1 (2019), e86.
de Solla, S., Gilroy, E.A., Klinck, J., King, L., McInnis, R., Struger, J., Backus, S., Gillis, P., 2016. Bioaccumulation of pharmaceuticals and personal care products in the unionid mussel Lasmigona costata in a river receiving wastewater effluent. Chemosphere 146, 486–496.
Dyck, J.R.B., Kudo, N., Barr, A.J., Davies, S.P., Hardie, D.G., Lopaschuk, G.D., 1999. Phosphorylation control of cardiac acetyl-CoA carboxylase by cAMP-dependent protein kinase and 5-AMP activated protein kinase. Eur. J. Biochem. 262, 184–190.
Ebele, A.J., Abdallah, M.A.E., Harrad, S., 2017. Pharmaceuticals and personal care products (PPCPs) in the freshwater aquatic environment. Emerg. Contam. 3 (1), 1–16.
Elmore, S., 2007. Apoptosis: a review of programmed cell death. Toxicol. Pathol. 35 (4), 495–516.
Finelli, M.J., Paramo, T., Pires, E., Ryan, B.J., Wade-Martins, R., Biggin, P., McCullagh, J., Oliver, P.L., 2019. Oxidation resistance 1 modulates glycolytic pathways in the cerebellum via an interaction with Glucose-6-Phosphate isomerase. Mol. Neurobiol. 56 (3), 1558–1577.
Garcia, D., Shaw, R.J., 2017. AMPK: mechanisms of cellular energy sensing and restoration of metabolic balance. Mol. Cell 66 (6), 789–800.
Ghoshdastidar, A.J., Fox, S., Tong, A.Z., 2015. The presence of the top prescribed pharmaceuticals in treated sewage effluents and receiving waters in Southwest Nova Scotia, Canada. Environ. Sci. Pollut. Res. 22, 689–700. https://doi.org/10.1007/s11356-014-3400-z.
Gong, L., Goswamic, S., Giacominic, K.M., Altmana, R.B., Klein, T.E., 2012. Metformin pathways: pharmacokinetics and pharmacodynamics. Am. J. Pharmacogenomics 22, 820–827. https://doi.org/10.1097/FPC.0b013e3283559b22.
Isenberg, J.S., Martin-Manso, G., Maxhimer, J.B., Roberts, D.D., 2009. Regulation of nitric oxide signalling by thrombospondin 1: implications for anti-angiogenic therapies. Nat. Rev. Cancer 9, 182–194. https://doi.org/10.1038/nrc2561.
Kim, E., Liu, N.C., Yu, I.C., Lin, H.Y., Lee, Y.F., Sparks, J.D., Chen, L.M., Chang, C., 2011. Metformin inhibits nuclear receptor TR4–MediatedHepatic Stearoyl-CoA desaturase 1 gene ExpressionWith altered insulin sensitivity. Diabetes 60, 1493–1503.
Leei Lin, B., Li, A., Young Mun, J., Previs, M.J., Beck Previs, S., Campbell, S.G., dos Remedios, C.G., Tombe, de P., Craig, R., Warshaw, D.M., Sadayappan, S., 2018. Skeletal myosin binding protein-C isoforms regulate thin filament activity in a Ca2+-dependent manner. Sci. Rep. 8, 2604. https://doi.org/10.1038/s41598-018-21053-1.
Li, Y., Xu, S., Mihaylova, M.M., Zheng, B., Hou, X., Jiang, B., Park, O., Luo, Z., Lefai, E., Shyy, J.Y., Gao, B., Wierzbicki, M., Verbeuren, T.J., Shaw, R.J., Cohen, R.A., Zang, M., 2011. AMPK phosphorylates and inhibits SREBP activity to attenuate hepatic steatosis and atherosclerosis in diet-induced insulin-resistant mice. Cell Metab. 13, 376–388.
Maclver, N.J., Jacobs, S.R., Wieman, H.L., Wofford, J.A., Coloff, J.L., Rathmell, J.C., 2008. Glucose metabolism in lymphocytes is a regulated process with significant effects on immune cell function and survival. J. Leukoc. Biol. 84, 949–957.
Markiewicz, M., Jungnickel, C., Stolte, S., Bialk-Bielinska, A., Kumirska, J., Mrozik, W., 2017. Ultimate biodegradability and ecotoxicity of orally administered antidiabetic drugs. J. Hazord Mat. 333, 154–161. https://doi.org/10.1016/j.jhazmat.2017.03.030.
Mihaylova, M.M., Shaw, R.J., 2011. The AMPK signalling pathway coordinates cell growth, autophagy and metabolism. Nat. Cell Biol. 13, 1016–1023. https://doi.org/10.1038/ncb2329.
Miyazaki, M., Kato, M., Tanaka, K., Tanaka, M., Kohjima, M., Nakamura, K., Enjoji, M., Nakamuta, M., Kotoh, K., Takayanagi, R., 2012. Increased hepatic expression of dipeptidyl peptidase-4 in non-alcoholic fatty liver disease and its association with insulin resistance and glucose metabolism. Mol. Med. Rep. 5, 729–733.
Muller, C., Herberth, H., Cosquer, B., Kelche, C., Cassel, J.C., Schimchowitsch, S., 2007. Structural and functional recovery elicited by combined putrescine and aminoguanidine treatment after aspirative lesion of the fimbria-fornix and overlying cortex in the adult rat. Eur. J. Neurosci. 25, 1949–1960.
Neely, A., Hidalgo, P., 2014. Structure-function of proteins interacting with the α1 pore-forming subunit of high-voltage-activated calcium channels. Front. Physiol. 5 (209), 1–19. https://doi.org/10.3389/fphys.2014.00209.
Oosterhuis, M., Sacher, F., ter Laak, T.L., 2013. Prediction of Concentration Levels of Metformin and Other High Consumption Pharmaceuticals in Wastewater and Regional Surface Water Based on Sales Data.
Ordovas, J.M., 2009. Genetic influences on blood lipids and cardiovascular disease risk: tools for primary prevention. Am. J. Clin. Nutr. 89 (5), 1509–1517.
Peek, S., Men Mah, K., Weinger, J.A., 2017. Regulation of neuronal circuit formation by protocadherins. Cell. Mol. Life Sci. 72 (22), 4133–4157.
Pentikäinen, P.J., Neuvonen, P.J., Penttilfi, A., Hc, I., 1979. Pharmacokinetics of metformin after intravenous and oral administration to man. Eur. J. Clin. Pharmacol. 202, 195–202.
Pernice, H.F., Schieweck, R., Jafari, M., Straub, T., Bilban, M., Kiebler, M.A., Popper, B., 2019. Altered glutamate receptor ionotropic Delta subunit 2 expression in Stau2-Deficient cerebellar purkinje cells in the adult brain. Int. J. Mol. Sci. 20 (7), 1797. https://doi.org/10.3390/ijms20071797.
Perry, D.K., Hannun, Y.A., 1998. The role of ceramide in cell signaling. Biochimica Et Biophysica Acta-Mol. Cell Biol. Lipids. 1436, 233–243.
Quick, A.P., Wang, Q., Philippen, L.E., Barreto-Torres, G., Chiang, D.Y., Beavers, D., Wang, G., Khalid, M., Reynolds, Jo, Campbell, H.M., Showell, J., McCauley, M.D., Scholten, A., Wehrens, X.H.T., 2017. Striated muscle preferentially expressed protein kinase' (SPEG) is essential for cardiac function by regulating junctional membrane complex activity. Circ. Res. 110–119. https://doi.org/10.1161/CIRCRESAHA.116.309977.
Rogers, N.M., Seeger, F., Garcin, E.D., Roberts, D.D., Isenberg, J.S., 2014. Regulation of soluble guanylate cyclase by matricellular thrombospondins: implications for blood flow. Front. Physiol. 5, 134. https://doi.org/10.3389/fphys.2014.00134.
Rotermund, C., Machetanz, G., Fitzgerald, J.C., 2018. The Therapeutic Potential of Metformin in Neurogenerative Diseases. Frontiers in Endocrinology . 9 (400), 1–26. https://doi.org/10.3389/fendo.2018.00400.
Scheurer, M., Michel, A., Brauch, H.J., Ruck, W., Sacher, F., 2012. Occurrence and fate of the antidiabetic drug metformin and its metabolite guanylurea in the environment and during drinking water treatment. Water Res. 46, 4790–4802. https://doi.org/10.1016/j.watres.2012.06.019.
Schmid, S.M., Kott, S., Sager, C., Huelsken, T., Hollmann, M., 2009. The glutamate receptor subunit delta2 is capable of gating its intrinsic ion channel as revealed by ligand binding domain transplantation. Proc. Natl. Acad. Sci. U.S.A. 106 (25), 10320–10325. https://doi.org/10.1073/pnas.0900329106.
Shahmohamadloo, RenéS., Simmons, Denina B.D., Sibley, Paul K., 2020. Shotgun proteomics analysis reveals sub-lethal effects in Daphnia magna exposed to cell-bound microcystins produced by Microcystis aeruginosa. Comp. Biochem. Physiol. Part D Genomics Proteomics 33, 100656.
Simmons, D.B.D., Bols, N.C., Duncker, B.P., McMaster, M.E., Miller, J., Sherry, J.P., 2012. Proteomic profiles of white sucker (Catostomus commersonii) sampled from within the Thunder Bay Area of concern reveal up-regulation of proteins associated with tumor formation and exposure to environmental estrogens. Environ. Sci. Technol. 46, 1886–1894.
Simmons, D.B.D., Miller, J., Clarence, S., McCallum, E.S., Balshine, S., Chandramouli, B., Cosgrove, J., Sherry, J.P., 2017. Altered expression of metabolites and proteins in wild and caged fish exposed to wastewater effluents in situ. Nature 7, 1–14. https://doi.org/10.1038/s41598-017-12473-6.
Stanton, R.C., 2012. Glucose-6-phosphate dehydrogenase, NADPH, and cell survival. IUBMB Life 64, 362–369. https://doi.org/10.1002/iub.1017.
Suwa, M., Egashira, T., Nakano, H., Sasaki, H., Kumgai, S., 2006. Metformin increases PGC-1α protein and oxidative enzyme activities possibly via AMPK phosphorylation in skeletal muscle in vivo. J. Appl. Physiol. 101, 1685–1692.
Tang, T., Lord, J.M., Norman, R.J., Yasmin, E., Balen, A.H., 2012. Insulin-sensitising drugs (metformin, rosiglitazone, pioglitazone, D- chiro-inositol) for women with polycystic ovary syndrome, oligo amenorrhoea and subfertility. CochraneDatabase System. Rev. (5) https://doi.org/10.1002/14651858.CD003053.pub5. Art. No.: CD003053.
Tisler, S., Zwiener, C., 2018. Formation and occurrence of transformation products of metformin in wastewater and surface water. Sci. Total Environ. 628, 1121–1129.
Toda, K., Kokushi, E., Uno, S., Shiiba, A., Hasunuma, H., Fushimi, Y., Wijayagunawardane, M.P.B., Zhang, C., Yamato, O., Taniguchi, M., Fink-Gremmels, J., Takagi, M., 2017. Gas chromatography-mass spectrometry for metabolite profiling of japanese black cattle naturally contaminated with zearalenone and sterigmatocystin. Toxins 9, 1–13.
Trautwein, C., Berset, D., Wolschke, H., 2014. Occurrence of the antidiabetic drug Metformin and its ultimate transformation product Guanylurea in several compartments of the aquatic cycle. Environ. Int. 70, 203–212. https://doi.org/10.1016/j.envint.2014.05.008.
Treves, S., Anderson, A.A., Ducreux, S., Divet, A., Bleunven, C., Grasso, C., Paesante, S., Zorzato, F., 2005. Ryanodine receptor 1 mutations, dysregulation of calcium homeostasis and neuromuscular disorders. Neuromuscul. Disord. 15, 577–578. https://doi.org/10.1016/j.nmd.2005.06.008.
Ussery, E., Bridges, K.N., Pandelides, Z., Kirkwood, A., Bonetta, D., Venables, B.J., Guchardi, J., Holdway, D., 2018. Effects of environmentally relevant metformin exposure on Japanese medaka (*Oryzias latipes*). Aquat. Toxicol. 205, 58–65.
Ussery, E., Bridges, K.N., Pandelides, Z., Kirkwood, A., Guchardi, J., Holdway, D., 2019. Developmental and full-life cycle exposures to guanylurea, and guanylurea-metformin mixtures results in adverse effects on Japanese medaka (Oryzias latipes). Environ. Tox Chem 38 (5), 1023–1028. https://doi.org/10.1002/etc.4403.
Vazquez-Arreguin, K., Maddox, J., Kang, J., Park, D., Cano, R.R., Factor, R.E., Ludwig, T., Tantin, D., 2018. BRCA1 through its E3 ligase activity regulates the transcription factor Oct1 and carbohydrate metabolism. Mol. Cancer Res. https://doi.org/10.1158/1541-7786.MCR-17-0364.
Vogt, M.C., Bruning, J.C., 2013. CNS insulin signaling in the control of energy homeostasis and glucose metabolism – from embryo to old age. Trends Endocrin Metab. 24 (2), 76–84. https://doi.org/10.1016/j.tem.2012.11.004.
Wakil, S.J., Abu-Elheiga, L.A., 2009. Fatty acid metabolism: target for metabolic syndrom. J. Lipid Res. (Suppl), S138–S143. https://doi.org/10.1194/jlr.R800079-JLR200.

Zagorska, A., 2010. New roles for the LKB1-NUAK pathway in controlling myosin phosphatase complexes and cell adhesion. Sci. Signal. 3, ra25.
Zhang, L., Ge, L., Parimoo, S., Stenn, K., Prouty, S.M., C, S.B.T.R, 1999. Human stearoyl-CoA desaturase: alternative transcripts generated from a single gene by usage of tandem polyadenylation sites. Biochem. J. 264, 255–264.
Ziegler, D.V., Wiley, C.D., Velarde, M.C., 2015. Mitochondrial effectors of cellular senescence: beyond the free radical theory of aging. Aging Cell 14 (1), 1–7.